A Study on the Forging of Gear-Like Components

Jongung Choi* Haeyong Cho, Jaechan Choi* and Changyong Jo*****

(*Received September 5, 1997*)

This paper describes kinematically admissible velocity fields for forging of gear-like components such as involute spur gear, trapezoidal spline, square spline, serration and trochoidal gear. Half pitch of each gear-like component was divided into several deformation zones with respect to their tooth profile. A neutral surface has been used to represent the inward flow of material during a forging operation by using a hollow billet with a flat punch. By using the suggested kinematically admissible velocity fields, the power requirements were successfully calculated and they were compared with experimental inspections. As a result, the suggested velocity fields are shown to be useful to predict the forging load. The contour of neutral surface varied with the number of teeth.

Key Words: Upper Bound Method, Velocity Field, Gear-Like Forging, Neutral Surface, Solid and Hollow Billet

Nomenclature

r, θ, z	: Cylindrical coordinate system
M	: Module, fillet and tooth radius [mm]
N	: Number of teeth
r_n	: Neutral surface radius [mm]
r_r	: Root circle radius [mm]
U	: Ram speed [mm/s]
$\dot{\bar{\varepsilon}}_i$	: Effective strain rate for i zone
σ	: Flow stress
Di/Do	: Ratio of inner to outer diameter of the initial billet
U_r, U_θ, U_z	: Velocity component
r_f	: Fillet circle radius [mm]
r_p	: Pitch circle radius [mm]
t	: Height of workpiece [mm]
α	: Half pitch angle [rad]
$\lvert\Delta V\rvert$	: Velocity discontinuity

* Dept. of Mechanical Design Engineering, Pusan National University, Pusan
** Dept. of Precision & Mechanical Engineering, Chungbuk National University, Cheongju
*** Korea Institute of Machinary & Materials, kyungnam.

1. Introduction

Gear-like components are widely used in the fields of automobile, aircraft and shipping etc. Two groups of manufacturing methods for gear-like components ; cutting and non-cutting one are available in engineering industry. Forging of gear-like components is one of the non-cutting methods. Its process has been developed recently [1-9] and complete filling up of materials into a die cavity is regarded as the most important factor to improve the dimensional accuracy. To achieve it, prediction of power requirement and relative pressure is a critical issue to be addressed in the forging process. Several upper bound solutions for gear-like components had been proposed to predict the forging load and relative pressure.

Juneja et al. (1984) and Kondo et al. (1985) analysed forging of spur gear by upper bound method. They assumed the tooth profile as trapezoidal one instead of involute tooth profile for a simplification of analysis. Abdul and Dean (1986) assumed the side of teeth as a straight line parallel to the center line of a tooth. Normal velocity is discontinuous on the shear surface in the analyses done by Juneja et al. (1984) and Kondo et al.

(1985). The velocity field proposed by Dean could not evaluate the boundary condition at the surface of the die. Cho et al. (1996) suggested the upper bound solution for a involute spur gear with solid and hollow billets and calculated the power requirements. As mentioned above, there are many reports about forging of gear-like components. However, they are limited to apply for only one type of tooth profile like gear or spline.

This paper proposes the velocity fields for forging of gear-like components. The forging loads are calculated from the suggested velocity fields by numerical calculation using solid and hollow billets with a flat punch. The calculated solutions are compared with experimental results.

2. Velocity Fields for Deformation Zone

The cylindrical coordinate system(r, θ, z) has been used in this analysis. Division of deformation zone is necessary for upper bound analysis. To do this, half pitch of gear-like components is divided into four parts as shown in Fig. 1. One is an axisymmetric part labeled Ⅰ. It is bounded by two planes of symmetry and a neutral surface. Using solid billets, this part is not needed. Another is an inner part labeled Ⅱ. This part has two subzones except serration and trochoidal gear. The third is a fillet part labeled Ⅲ which exists in involute spur gear. The fourth is a tooth part labeled Ⅳ. During forging process, material fills up to this part.

Throughout the analysis, the following assumptions are employed. (1) The shape of free flow surface is a circle centered at the gear center O. (2) The constant friction factor is considered on the interface of die/workpiece. (3) The outer diameter of a billet is equal to that of a root circle. (4) The material is homogeneous and rigid-plastic. The kinematically admissible velocity field of the workpiece should satisfy the volume constancy and the boundary condition ; On the surface of workpiece, the material should not flow across the die surface. Assuming that the punch moves downward at unit velocity, the axial velocity U_z and the axial strain rate are given by as the following equation.

$$U_z=-\frac{u}{t}Z \tag{1}$$

Here, t represents the height of workpiece and z is the axial coordinate.

2.1 Velocity fields for axisymmetric part

A) For deformation zone Ⅰ

This zone is bounded by two symmetric planes, a neutral surface and an inner surface as shown in Fig. 1. In this zone, we assume that the circumferential velocity and radial velocity(at $r=r_n$) are zero. The velocity field for this zone is given as follows :

$$U_r=\frac{u}{2t}\left(r-\frac{r_n^2}{r}\right),\ U_\theta=0$$

Using solid billets, the inner surface does not exist and this zone is not needed.

2.2 Velocity fields for inner part

A) For deformation zone Ⅱ-1

In this zone, the workpiece contacts with the die surface FG, so we assume that the radial velocity is zero. The velocity field for this zone is given as follows :

$$U_r=0,\ U_\theta=\frac{u}{t}r\theta$$

B) For deformation zone Ⅱ-2

At the boundary of this zone, we assume that the circumferential velocity $U_{\theta,II-1}=U_{\theta,II-2}$ where $\theta=\theta_1$, $U_{\theta,II-2}=0$ where $\theta=0$ and the radial velocity $U_{r,II-1}=U_{r,II-2}=0$ where $r=r_n$. The velocity field for this zone is given as follows :

$$U_r=\frac{u}{2t}\left(r-\frac{r_n^2}{r}\right)\left(\frac{\alpha}{\alpha-\theta_1}\right),$$

$$U_\theta=\frac{ur}{t}\frac{\theta_1}{\alpha-\theta_1}(\alpha-\theta)$$

As shown in Fig. 1(d), (e), if Ⅱ-1 zone is not needed, the velocity fields for this zone is given as follow :

$$U_r=\frac{u}{2t}\left(r-\frac{r_n^2}{r}\right),\ U_\theta=0$$

2.3 Velocity fields for fillet part

A) For deformation zone Ⅲ-1

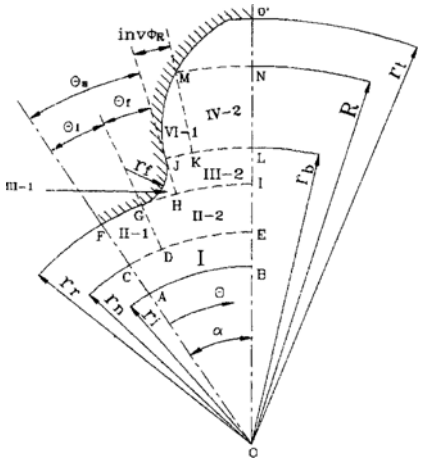

(a) Involute spur gear

The boundary condition in this zone is that the normal velocity to the die surface should be zero. The velocity field for this zone is given as follows :

$$U_r=\frac{u\cdot r}{2t}+\frac{C_{III-1}}{r},\quad U_\theta=\left(\frac{u\cdot r}{2t}+\frac{C_{III-1}}{r}\right)\cot\varphi$$

Where, $C_{III-1}=\frac{ur_r^2}{2t}\left(\frac{\theta_1}{\alpha-\theta_1}\right)+\frac{ur_n^2}{2t}\left(\frac{\alpha}{\alpha-\theta_1}\right)$ and $\cot\varphi$ should be expressed as the function of radius r as the following equation.

$$\cot\varphi=\frac{(r_r+r_f)^4-(r^2-r_f^2)^2-(r^2-r_r^2)\left[(2r_f+r_r)^2-r^2\right]}{2(r_r+r_f)^2\sqrt{(r^2-r_r^2)\left[(2r_f+r_r)^2-r^2\right]}}$$

B) For deformation zone Ⅲ-2

The boundary conditions for this zone is that

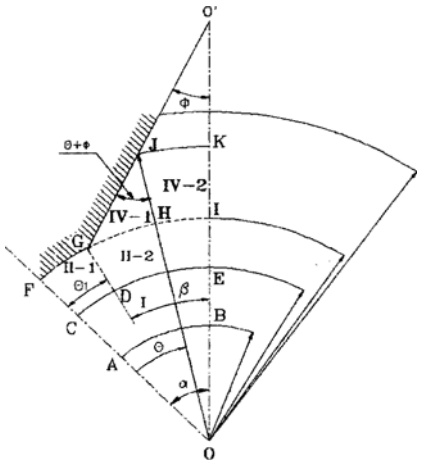

(b) Trapezoidal spline

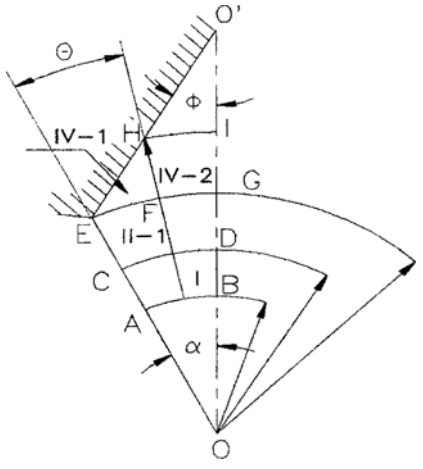

(d) Serration

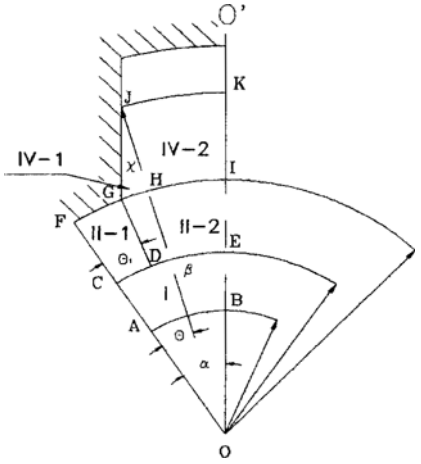

(c) Square spline

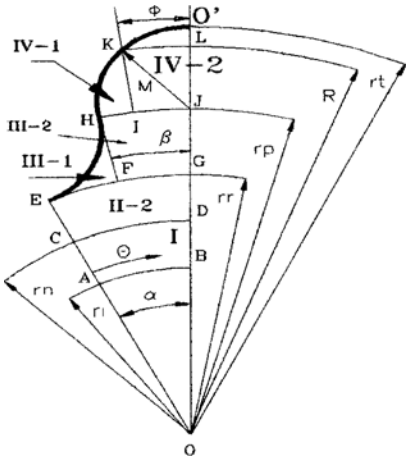

(e) Trochoidal gear

Fig. 1 Schematic drawing of half pitch for each components.

$U_{\theta,V}=U_{\theta,VI}$ for $\theta=\theta_S$ and $U_\theta=0$ for $\theta=\alpha$. So we can assume that the circumferential velocity is distributed as a linear function of angle θ. The velocity field for this zone is given as follows :

$$U_r=\frac{ur}{2t}+\frac{C_1}{2tr(\alpha-\theta_1)}+\frac{C_{IV}}{\alpha-\theta_s}\frac{C_2}{r}+\frac{C_{III-2}}{r},$$

$$U_\theta=\frac{\alpha-\theta}{\alpha-\theta_s}\left(\frac{ur}{2t}+\frac{C_{III-2}}{r}\right)\cot\varphi$$

$$C_1=\frac{1}{2}\sqrt{(r^2-r_r^2)\left[(2r_f+r_r)^2-r^2\right]}+2r_f^2\sin^{-1}\left(\frac{\sqrt{(2r_f+r_r)^2-r^2}}{2\sqrt{r_f(r_r+r_f)}}\right)$$

$$C_2=\frac{1}{2}(\tan^{-1}A+\tan^{-1}B)+\sin^{-1}\left(\frac{\sqrt{(2r_f+r_r)^2-r^2}}{2\sqrt{r_f(r_r+r_f)}}\right)-\frac{\sqrt{(r^2-r_r^2)\left[(2r_f+r_r)^2-r^2\right]}}{4(r_r+r_f)^2}$$

$$A=-\frac{(2r_f+r_r)\sqrt{(2r_f+r_r)^2-r^2}+4r_f(r_r+r_f)}{r_r(r^2-r_r^2)}$$

$$B=-\frac{(2r_f+r_r)\sqrt{(2r_f+r_r)^2-r^2}-4r_f(r_r+r_f)}{r_r(r^2-r_r^2)}$$

2.4 Velocity fields for tooth part

A) For deformation zone Ⅳ-1

The workpiece contacts with the die surface as shown in Fig. 1. The normal velocity to the die surface should be zero. The circumferential velocity on the involute curve could be assumed as a function of radius r only and it is a function of two variables, radius r and angle θ in the deforming zone. The velocity fields for each tooth shape are given as follows :

① involute spur gear : $U_\theta=U_r(\theta-\theta_s+\phi_r)$
② trapezoidal spline : $U_\theta=U_r\tan\gamma$
③ square spline : $U_\theta=U_r\tan\chi$
④ serration : $U_\theta=U_r\tan\gamma$
⑤ trochoidal gear : $U_\theta=U_r\cdot\dfrac{r^2-a\cdot b}{\sqrt{(a^2-r^2)(r^2-b^2)}}$

where, $\phi_r=\tan^{-1}\dfrac{\sqrt{r^2-r_b^2}}{r_b}$, $\gamma=\cos^{-1}\cdot\dfrac{\sqrt{r^2-\overline{OO'}^2\sin^2\phi}}{r}$,

$$\chi=\sin^{-1}\left[\frac{r_r}{r}\sin\beta\right],\ a=r_p+M,\ b=r_p-M.$$

By using these equations and volume constancy, the velocity components for each direction are given as follows :

① involute spur gear : $U_r=\dfrac{ur}{3t}+\dfrac{C_{IV-1}}{r^2}$,

$$U_\theta=\left(\frac{ur}{3t}+\frac{C_{IV-1}}{r^2}\right)(\theta-\theta_s+\phi_r)$$

② trapezoidal spline : $U_r=\dfrac{ur}{2t}+\dfrac{C_{IV-1}}{r}$,

$$U_\theta=\left(\frac{ur}{2t}+\frac{C_{IV-1}}{r}\right)\tan\gamma$$

③ square spline : $U_r=\dfrac{ur}{2t}+\dfrac{C_{IV-1}}{r}$,

$$U_\theta=\left(\frac{ur}{2t}+\frac{C_{IV-1}}{r}\right)\tan\chi$$

④ serration : $U_r=\dfrac{ur}{2t}+\dfrac{C_{IV-1}}{r}$,

$$U_\theta=\left(\frac{ur}{2t}+\frac{C_{IV-1}}{r}\right)\tan\gamma$$

⑤ trochoidal gear : $U_r=\dfrac{ur}{2t}+\dfrac{C_{IV-1}}{r}$,

$$U_\theta=\left(\frac{ur}{2t}+\frac{C_{IV-1}}{r}\right)\frac{r^2-a\cdot b}{\sqrt{(a^2-r^2)(r^2-b^2)}}$$

Where, C_{IV-1} is a constant value determined by the boundary condition. As shown in the above equations, velocity fields for gear-like components are functions of tooth profile only.

B) For deformation zone Ⅳ-2

We can assume that the circumferential velocity is distributed as a linear function of angle θ. The radial velocity component should be zero on the symmetric plane. By the assumption and the boundary condition, the velocity fields for this zone are given as follows :

① involute spur gear

$$U_r=\frac{ur}{2t}+C_R\left(\frac{ur}{6t}-\frac{C_{IV-1}}{r^2}\right)+C_R''\left[\frac{u}{3t}\left(\frac{r}{2}\tan^{-1}R_{con}-\frac{r_b}{2r}R_{con}\right)+C_{IV-1}\left(-\frac{1}{r}\tan^{-1}R_{con}+\frac{R_{cen}}{r^2}\right)\right]+\frac{C_{IV-2}}{r}$$

$$U_\theta=\frac{\alpha-\theta}{\alpha-(\theta_s+inv\phi_R)}\left(\frac{ur}{3t}+\frac{C_{IV-1}}{r^2}\right)(inv\phi_R+\phi_r)$$

Where, $R_{con}=\dfrac{\sqrt{r^2-r_b^2}}{r_b}$,

$$C_R=\frac{inv\phi_R}{\alpha-(\theta_s+inv\phi_R)},\quad C_R''=\frac{1}{\alpha-(\theta_s+inv\phi_R}$$

$$C_{IV-2}=\frac{1}{\alpha-\theta_s}\frac{C_1''}{2t}+\frac{C_{III-1}\cdot C_2''}{\alpha-\theta_s}+C_{III-2}-C_R\left(\frac{ur_b^2}{6t}-\frac{C_{IV-1}}{r_b^2}\right)$$

$$inv\phi_R=\frac{\sqrt{R^2-r_b^2}}{r_b}-\tan^{-1}\frac{\sqrt{R^2-r_b^2}}{r_b}$$

② trapezoidal spline

$$U_r=\frac{ur}{2t}-\frac{uC_L}{2tr(\beta-\phi)}\sqrt{r^2-C_L^2}+\frac{C_{IV-1}}{(\beta-\phi)}\tan^{-1}\left(\frac{a}{\sqrt{r^2-C_L^2}}\right)+\frac{C_{IV-2}}{r}$$

$$U_\theta=\left(\frac{ur}{2t}+\frac{C_{IV-1}}{r}\right)\frac{\theta}{\beta-\phi}\tan\gamma$$

Where, $C_L=\overline{OO''}\sin\phi$

③ square spline

$$U_r=\frac{ur}{2t}+\frac{C_{IV-1}}{(\beta-\varphi)r}\sin^{-1}\left(\frac{r_r}{r}\sin\beta\right)+\frac{C_{IV-2}}{r}-\frac{u}{2t(\beta-\varphi)}\left(\frac{r_r}{r}\sin\beta\sqrt{r^2-r_r^2\sin^2\beta}\right)$$

$$U_\theta=\frac{\theta}{\beta-\varphi}\left(\frac{ur}{2t}+\frac{C_{IV-1}}{r}\right)\tan\chi$$

⑤ trochoidal gear

$$U_r=\frac{u\cdot r}{2t}+\frac{u}{2tr}\frac{C_3}{\phi}+\frac{C_{IV-2}}{r}\cdot\frac{C_4}{\phi}+\frac{C_{IV-2}}{r},$$

$$U_\theta=\frac{\theta}{\phi}\left(\frac{u\cdot r}{2t}+\frac{C_{IV-2}}{r}\right)\frac{r^2-a\cdot b}{\sqrt{(a^2-r^2)(r^2-b^2)}}$$

Where, $C_3=\frac{\sqrt{(a^2-r^2)(r^2-b^2)}}{2}+\frac{(b-a)^2}{2}\sin^{-1}\sqrt{\frac{a^2-r^2}{a^2-b^2}}$

$$C_4=\sin^{-1}\sqrt{\frac{a^2-r^2}{a^2-b^2}}-\frac{1}{2}(\tan^{-1}C_k-\tan^{-1}D_k)$$

$$C_k=\frac{(b^2-a^2-a\sqrt{a^2-r^2})\cdot\sqrt{r^2-b^2}}{b(b^2-r^2)},$$

$$D_k=\frac{(b^2-a^2+a\sqrt{a^2-r^2})\cdot\sqrt{r^2-b^2}}{b(b^2-r^2)}$$

3. Results and Discussions

A kinematically admissible velocity field for forging of gear-like components has been proposed. Relative average punch pressures were determined. For each component, the thickness of product is 10 mm, the height of tooth is 2.25M and constant friction factors are considered. The upper bound solutions were compared with experimental results. All analyses were performed by using mechanical properties of Al 2024 and Al 2218 aluminum alloy. The flow stress at room temperature was modeled with the Ludwik-Hollomon equations :

$$\bar{\sigma}=358.00(\bar{\varepsilon})^{0.156}\ [\mathrm{MPa}],$$
$$\bar{\sigma}=352.48(\bar{\varepsilon})^{0.232}\ [\mathrm{MPa}]$$

The calculated solutions for three components were compared with experimental inspections. By using Al 2024 alloy, forging load of involute spur gear with number of 15 teeth was plotted versus height reduction as shown in Fig. 2. In Figs. 3 and 4, forging loads of trapezoidal spline and trochoidal gear with 12 teeth by using Al 2218 were plotted, respectively. At the final step, the calculated loads are higher than those of the experiment. This means that the solutions from the proposed velocity fields are useful to determine the capacity of forging equipment. As shown in the figures, there are differences in height reduction between theoretical and experi-

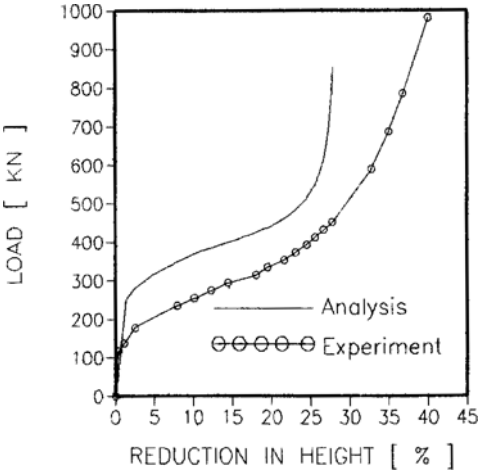

(a) Solid involute gear

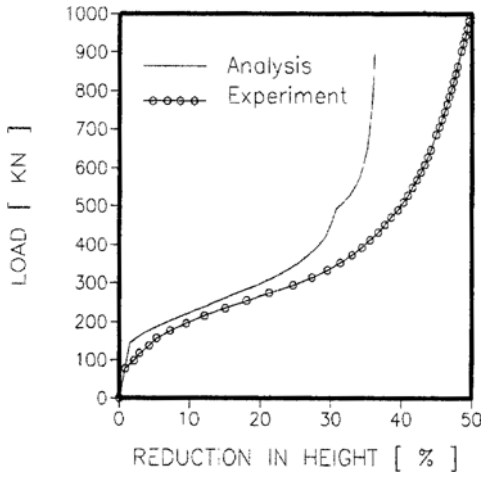

(b) Hollow involute gear

Fig. 2 Comparison of load between analysis and experiment for involute spur gear.

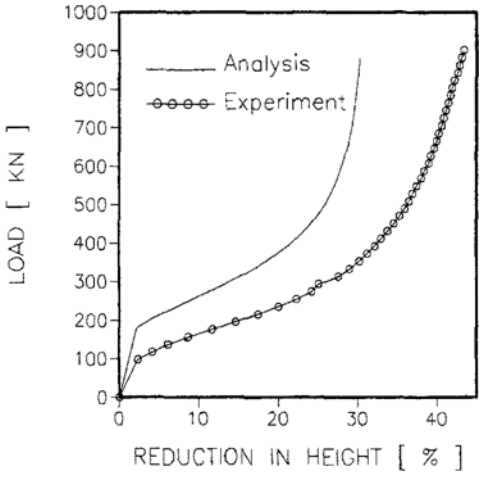

(a) Solid trapezoidal spline

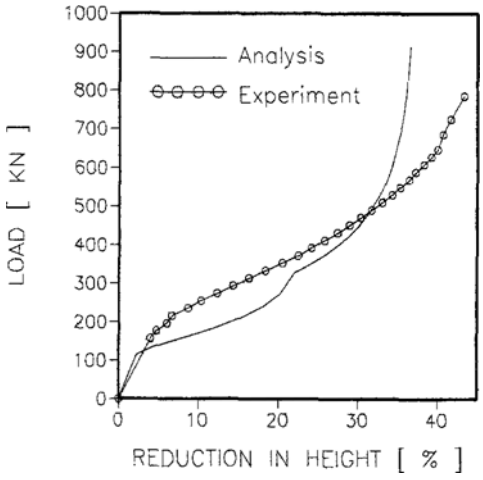

(b) Hollow trapezoidal spline

Fig. 3 Comparison of load between analysis and experiment for trapezoidal spline.

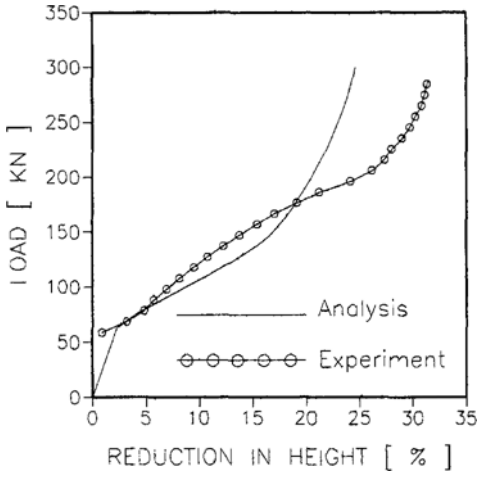

(a) Solid trochoidal gear

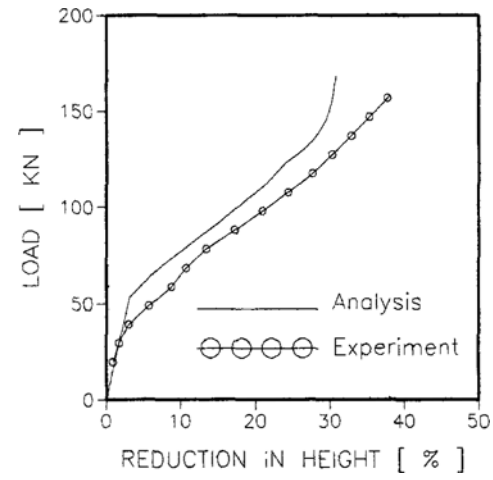

(b) Hollow trochoidal gear

Fig. 4 Comparison of load between analysis and experiment for trochoidal gear.

mental results. It seems to be caused by elastic deformation of the die, elastic spring back of the workpiece and backward extrusion through the clearance between the die and the punch. The backward extrusion is the most likely cause of the difference. The inner radius of hollow billets varied during forging operation. The inner radii of analyses and experiments decrease during the forging process as shown in Fig. 5. The variation of inner radius, which was determined by the location of a neutral surface, is well predicted by the proposed approach. If the ratio of diameter (Di/Do) is small, the inner hole is closed at the final step as shown in the Fig. 6. At the final step, the load of a hollow billet is lower than that of a solid billet as shown in Figs. 2, 3 and 4. Thus, the larger inner radius of a billet would lead to less forging load. Based on the above finding, the maximum initial inner radius without buckling is recommended to reduce the forging load.

In Fig. 7, calculated solutions were compared with experimental results for forging of square spline with 6 teeth by using hollow and solid billets of Al 2218. The calculated load is higher than that of experiment until 10% height reduction, but as the height reduction exceeds 10%, the

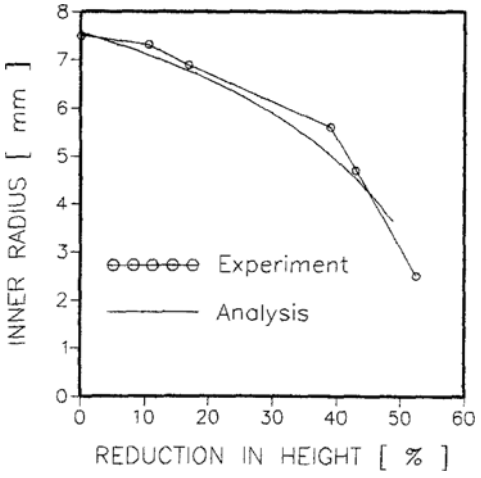

Fig. 5 Variations of inner and neutral radius during forging with hollow billet.

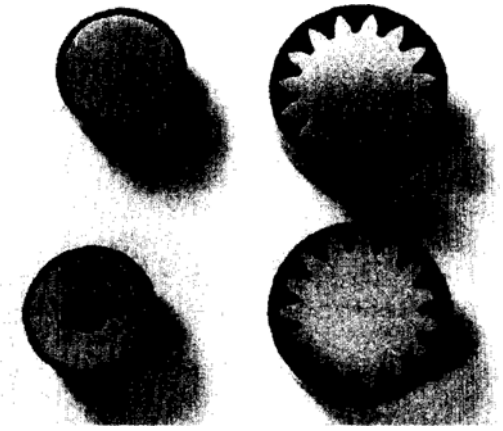

Fig. 6 Photographs of forged solid and hollow spur gear.

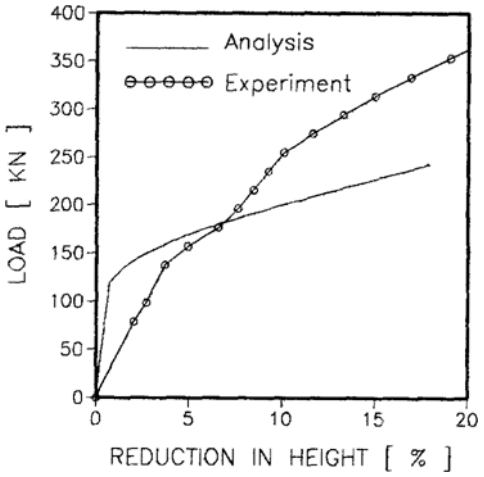

(a) Solid square spline

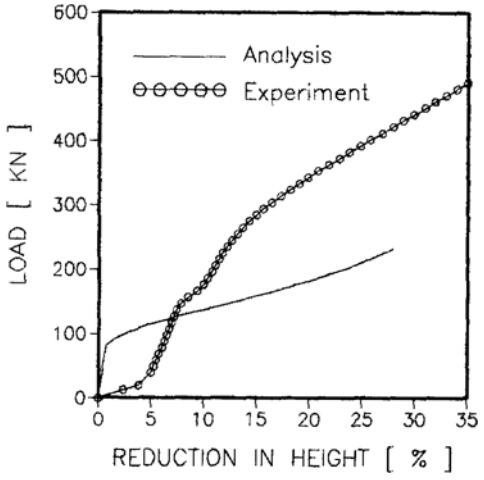

(b) Hollow square spline

Fig. 7 Comparison of load between analysis and experiment for square spline.

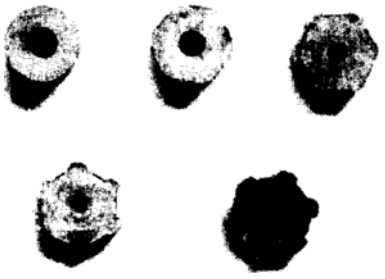

Fig. 8 Photographs of forged square spline for each step.

calculated load becomes lower. It seems that the difference in the shape of free flow surface between analysis and experiment is the cause of the aforementioned result. Actual shape of free flow surface is hyperbolic. while the ene used in the analysis is a circle centered at gear center O. This discrepancy is more serious for forging of a component with smaller ratio of tooth height to width (h/w) such as a square spline. Therefore, the free flow surface may be assumed as a circle only for forging of component with the large h/w ratio.

It was shown that forged square splines by using a hollow billet with 6 teeth in Fig. 8. The inner radius was reduced by the metal flow toward the center of half pitch. If the number of

teeth is small, the neutral surface profile is not a circle but a polygon and cracks were observed inside the surface of the workpiece. that the cracks seems to be initiated by stress concentration at apexes of the polygon corresponding to the symmetric plane. The suggested upper bound analysis is useful to predict the forging load of large the number of teeth. For forging of the small number of teeth, it is better to assume the neutral surface as a polygon with apexes that are same with the number of teeth. To fill up the die cavity, extrusion is more effective than forging to produce a component with small ratio of tooth height to width such as square spline.

4. Conclusion

The kinematically admissible velocity has been proposed for forging of gear-like components. By using the suggested method, the velocity fields have been proposed and numerical calculation program was established. From numerical calculations and experimental inspections, following conclusions can be drawn :

(1) The kinematically admissible velocity fields for forging of gear-like components by using solid and hollow cylindrical billets have been proposed. From the suggested method, the velocity fields for each shape have been derived.

(2) For the large ratio of tooth height to width, the calculated results from the proposed velocity fields are in good agreement with the experimental one. To fill up the die cavity for the small ratio of tooth height to width such as a square spline, extrusion is more effective than forging.

(3) For components with large the number of teeth, it was found that the neutral surface was assumed as a circle. For the small number of teeth, it was found that the neutral surface is a polygon with apexes that are same with teeth in number.

(4) For forging of components with the small ratio of tooth height to width, the shape of free flow surface has to be considered as a curve whose center velocity is faster than that of side.

Acknowledgment

The authors would like to thanks the support of ERC for Net-Shape and Die Manufacturing during this study.

References

Abdul-Rahman, A. R. O. and Dean, T. A. 1981 "The Quality of Hot Forged Spur Gear Forms. Part Ⅰ : Technical and Metallurgical Properties," *Int. J. Mach. Tool Des. Res.*, Vol. 21, No. 2, pp. 109～127

Abdul, N. A., and Dean, T. A., 1984 "An Analysis of the Forging of Spur Gear Forms," *Int. J. Mach. Tool Des. Res.*, Vol. 26, No. 2, pp. 113～123

Cho, H. Y., Choi, J. C., Choi, J. U. and Min, G. S., 1996, "An Upper Bound Analysis for Forging of Spur Gears," *Int. J. of Mechanical Science*, (submitted in 1996)

Choi, J. C., Cho, H. Y. and Kwon, H. H., 1993 "A new extrusion process of helical gears : experimental study," *J. Mat. Proc. Tech.*, Vol. 44, p. 35

Dohmann, F. and Traudt, O., 1987 "Metal Flow and Tool Stress in Cold Forging of Gear Components," *Advanced Technology of Plasticity*, Ⅱ, pp. 1081～1089

Fujikawa, S., Yoshioka, H. and Shimamura, S., 1992 "Cold-and Warm-Forging Applications in the Automotive Industry," *J. Mat. Proc. Tech.*, Vol. 35, pp. 317～342

Grover, O. P. and Juneja, B. L., 1984 "Analysis of Closed-Die Forging of Gear-Like Elements," *Advanced Technology of Plasticity*, Ⅱ, pp. 888～893

Moriguchi, I., 1992 "Cold Forging of Gear and Other Complex Shapes," *Journal of Materials Processing Technology*, Vol. 35, p. 439

Ohga, K., Kondo, K. and Jitsunari, T., 1985 "Research on Precision Die Forging Utilizing Divided Flow," *Bulletin of JSME*, Vol. 28, No. 244, pp. 2451～2459

Samanta, S. K., 1976 "Helical Gear : A Novel Method of Manufacturing It," *NAMRC*, pp. 199～205

Yang, D. Y., 1994 "Investigation in to Non-Steady State 3-Dimensional Extrusion of a Trochoidal Helical Gear by Rigid Plastic Finite Element Method," *Annals of the CIRP*, Vol. 13, No. 1, pp. 229~233